

## ***PPP1R14A* is Associated with Immunotherapy Resistance in Head and Neck Squamous Cell Carcinoma Identified by Single-Cell and Bulk RNA-Sequencing**

Jun-Jie Ma<sup>1#</sup>, Lei Zhang<sup>2#</sup>, Jin Lu<sup>3,4</sup>, Hao-Xuan Zhang<sup>3,4\*</sup>

<sup>1</sup>Department of Clinical Medicine, <sup>3</sup>Department of Human Anatomy, <sup>4</sup>Anhui Key Laboratory of Computational Medicine and Intelligent Health, Bengbu Medical University, Bengbu 233030, Anhui, China

<sup>2</sup>Department of General Surgery, The Second Affiliated Hospital of Bengbu Medical University, Bengbu 233030, Anhui, China

### **ABSTRACT**

**Objective** To identify nivolumab resistance-related genes in patients with head and neck squamous cell carcinoma (HNSCC) using single-cell and bulk RNA-sequencing data.

**Methods** The single-cell and bulk RNA-sequencing data downloaded from the Gene Expression Omnibus database were analyzed to screen out differentially expressed genes (DEGs) between nivolumab resistant and nivolumab sensitive patients using R software. The Least Absolute Shrinkage Selection Operator (LASSO) regression and Recursive Feature Elimination (RFE) algorithm were performed to identify key genes associated with nivolumab resistance. Functional enrichment of DEGs was analyzed with Gene Ontology and Kyoto Encyclopedia of Genes and Genomes analyses. The relationships of key genes with immune cell infiltration, differentiation trajectory, dynamic gene expression profiles, and ligand-receptor interaction were explored.

**Results** We found 83 DEGs. They were mainly enriched in T-cell differentiation, PD-1 and PD-L1 checkpoint, and T-cell receptor pathways. Among six key genes identified using machine learning algorithms, only *PPP1R14A* gene was differentially expressed between the nivolumab resistant and nivolumab sensitive groups both before and after immunotherapy ( $P < 0.05$ ). The high *PPP1R14A* gene expression group had lower immune score ( $P < 0.01$ ), higher expression of immunosuppressive factors (such as *PDCD1*, *CTLA4*, and *PDCD1LG2*) ( $r > 0$ ,  $P < 0.05$ ), lower differentiation of infiltrated immune cells ( $P < 0.05$ ), and a higher degree of interaction between HLA and CD4 ( $P < 0.05$ ).

**Conclusions** *PPP1R14A* gene is closely associated with resistance to nivolumab in HNSCC patients. Therefore, *PPP1R14A* may be a target to ameliorate nivolumab resistance of HNSCC patients.

**Key words:** *PPP1R14A*; head and neck squamous cell carcinoma; immunotherapy; drug resistance

### **INTRODUCTION**

Head and neck squamous cell carcinoma (HNSCC) is the sixth most common cancer in the world, and its incidence and mortality are increasing year by year<sup>[1]</sup>. The treatment modalities for HNSCC usually involve surgical resection, adjuvant radiotherapy, or a combination of radiotherapy and chemotherapy. The 5-year survival of HNSCC patients is less than 50% because about 60% of the patients are in advanced stages at diagnosis and the tumor are prone to lymph node

Received March 4, 2024; accepted April 18, 2024; published online June 18, 2024.

<sup>#</sup>Contributed equally to this work.

\*Corresponding author E-mail: zhxww@foxmail.com

© The authors 2024. Published by Chinese Academy of Medical Sciences. This is an open access article attributed under the CC BY-NC license (<http://creativecommons.org/licenses/by-nc/4.0/>).

metastasis and local recurrence<sup>[2,3]</sup>. In addition, surgery may lead to pharyngeal dysfunction or a defective head and neck appearance, and radiotherapy may result in damage to other organs, therefore leading to a poor clinical prognosis<sup>[4]</sup>. Fortunately, immune checkpoint inhibitors targeting programmed cell death protein 1 (PD-1) and programmed cell death protein ligand 1 (PD-L1) offer a treatment intensification strategy for patients with advanced or metastatic HNSCC, with the advantage of avoiding the side effects of conventional therapies and generating a sustained anti-tumor immune response<sup>[5]</sup>. They can effectively manipulate the immune system to specifically recognize and attack cancer cells. Nivolumab, an anti-PD-1 immune checkpoint inhibitor, has been approved for recurrent or metastatic HNSCC treatment. Although nivolumab improved overall and progression-free survivals, drug resistance compromises its efficacy<sup>[6,7]</sup>. There is a need to explore the resistance mechanisms to nivolumab. Therefore, we analyzed single-cell and bulk RNA-sequencing data using bioinformatics to identify possible genes that may be involved in nivolumab resistance to improve response rate and survival of HNSCC.

## MATERIALS AND METHODS

### Data acquisition

Sequencing data of HNSCC patients treated with nivolumab were downloaded from the Gene Expression Omnibus (GEO) database (<https://www.ncbi.nlm.nih.gov/geo/>). GSE195832 dataset contained RNA-sequencing data of tumor tissues from 96 HNSCC patients treated with nivolumab, of which 42 patients were sensitive to nivolumab and 54 resistant to nivolumab. GSE232240 dataset contained single-cell RNA-sequencing data of immune-infiltrating cells from tumor tissues in 18 HNSCC patients treated with nivolumab, of which 11 patients were sensitive and 7 resistant to nivolumab. The single-cell data were processed according to the following criteria: (1) retention of cells expressing between 1,000 and 100,000 genes; (2) retention of cells with less than 20% mitochondrial genes; and (3) retention of genes expressed between 500 and 10,000.

### Differential expression analysis of nivolumab resistance-related genes

For bulk data, differentially expressed genes (DEGs) between the nivolumab resistant and nivolumab sensitive patients were identified by "limma" package of R soft-

ware<sup>[8]</sup> with the criteria of false discovery rate (FDR) < 0.05 and log fold change (logFC) > 0. For single-cell data, resistance-associated DEGs (FDR < 0.05 and logFC > 0) were screened by "FindMarkers" function of "seurat" package<sup>[9]</sup>. Genes with an average logFC > 0.585 for both bulk and single-cell RNA-sequencing datasets were finally considered as nivolumab resistance-associated DEGs. Then, resistance scores of these DEGs were calculated by "UCell" package and used to explore the differential expression of DEGs in different cell types<sup>[10]</sup>.

### Functional enrichment analysis

Gene ontology (GO) and Kyoto Encyclopedia of Genes and Genomes (KEGG) enrichment analyses were performed to analyze the function of resistance-associated DEGs using the "clusterProfiler" package<sup>[11]</sup>. Gene set enrichment analysis (GSEA) was performed to identify biological function of DEGs<sup>[12]</sup>. Gene set variation analysis (GSVA) was used to estimate the enrichment scores of KEGG metabolism-related pathways of DEGs in patients resistant to nivolumab treatment<sup>[13]</sup>.

### Identification of DEGs associated with nivolumab resistance

The Least Absolute Shrinkage and Selection Operator (LASSO) regression and Recursive Feature Elimination (RFE) algorithm analyses<sup>[14,15]</sup> were utilized to screen the key genes related to nivolumab resistance. Next, an overlap of DEGs between the two datasets was identified using a Venn diagram web tool (<http://bioinformatics.psb.ugent.be/webtools/Venn/>).

### Evaluation of immune response

The CIBERSORT algorithm was used to calculate the level of immune cell infiltration in bulk RNA-sequencing data<sup>[16]</sup>. The ESTIMATE algorithm was used to estimate the immune score and tumor purity of each sample of bulk RNA-sequencing data<sup>[17]</sup>.

The correlation between the expression of *PPP1R14A* gene and different immunomodulatory factors was analyzed and logFC values and odds ratio (OR) values were obtained.

### Pseudotime and cellular communication analysis

The stemness score of each cell was calculated using the "CytoTRACE" software package<sup>[18]</sup>, and the CytoTRACE results were used to assist the "Monocle3" algorithm<sup>[19]</sup> to infer the proposed temporal differentiation trajectory of cells.

The tumor microenvironment is involved in complex intercellular communication. Exploring receptor-ligand interactions has a key role to reveal the tumorigenesis and development of drug resistance<sup>[20]</sup>. Therefore, the intensity of receptor-ligand interactions in different *PPP1R14A* expression groups was calculated by using "CellChat" software package<sup>[21]</sup> to evaluate the potential relationship between *PPP1R14A* expression and nivolumab resistance.

### Drug sensitivity analysis

To predict potential treatment sensitive drugs for nivolumab-resistant patients, we performed drug sensitivity analysis using data from the Genomics of Drug Sensitivity in Cancer (GDSC) database (<https://www.cancerxgene.org/>). The half maximal inhibitory concentration (IC50) of 565 drugs was assessed using the "oncoPredict" package<sup>[22]</sup> (for bulk sequencing data) and using the "beyondcell" package<sup>[23]</sup> (for single-cell sequencing data).

### Expression validation of key gene

GSE212551 dataset (including 76 resistant patients and 24 sensitive patients) and GSE226134 dataset (including 40 resistant patients and 9 sensitive patients) were used as external validation datasets to validate the expression of *PPP1R14A* gene between nivolumab sensitive and resistant patients.

In addition, we validated *PPP1R14A* expression between nivolumab sensitive and resistant HNSCC patients ( $n = 522$ ) in The Cancer Genomic Atlas (TCGA, <https://portal.gdc.cancer.gov/>) using the Tumor Immune Dysfunction and Exclusion (TIDE) algorithm<sup>[24]</sup>.

### Statistical analysis

All statistical analyses were performed by using R (version 4.3.1, <https://www.r-project.org/>). Data were described as mean  $\pm$  standard deviation (SD) or median and interquartile range (IQR). The differences between variables of different groups were tested using Wilcoxon test. Correlation analysis was performed using Spearman correlation test.  $P < 0.05$  was considered statistically significant.

## RESULTS

### DEGs associated with nivolumab resistance

We found 83 genes highly expressed in the nivolumab-resistant group by analyzing bulk and single-cell RNA-

sequencing data ( $\log_{2}FC > 0.585$ ,  $FDR < 0.05$ , **Fig. 1A**). GO analysis showed that the biological process of these DEGs was mainly enriched in pathways such as regulation of T cell differentiation, Th2 cell differentiation, and RNA modification. The main cellular components were inner mitochondrial membrane, mitochondrial matrix, and mitochondrial ribosomes. Molecular function focused on tumor necrosis factor binding, membrane insertion enzyme activity, and glucokinase activity. KEGG analysis showed that these DEGs were mainly enriched in PD-1 and PD-L1 checkpoint pathway, T-cell receptor signaling pathway, and tumor necrosis factor (TNF) signaling pathway (**Fig. 1B**). Moreover, pathways mediating T cell receptor activity were inhibited, whereas pathways regulating NK cell-mediated cytotoxicity were activated (**Fig. 1C**). Resistance scores for DEGs were highest in plasmacytoid dendritic cells (pDC) and lowest in conventional dendritic cells (cDC) (**Fig. 1D-1F**).

### Key genes for nivolumab resistance

LASSO regression screened out 10 key genes for drug resistance (**Fig. 2A**). For its minimum prediction error, random forest model of RFE algorithm was chosen for analysis, and screened out 35 key genes (**Fig. 2B**). Subsequently, through overlapping DEGs of bulk and single-cell RNA-sequencing datasets, 6 key genes were identified, including FKBP prolyl isomerase 1B (*FKBP1B*), MHC class I polypeptide-related sequence A (*MICA*), peptidyl arginine deiminase 4 (*PADI4*), protein phosphatase 1 regulatory inhibitor subunit 14A (*PPP1R14A*), SNRPN upstream open reading frame (*SNURF*), and TraB domain 2A (*TRABD2A*) (**Fig. 2C**).

Furthermore, we found that regardless of before and after nivolumab treatment, only *PPP1R14A* among the six key genes had statistically significant expression levels between the resistant group and the sensitive group, with a decrease in expression after treatment in the sensitive group and an increase in expression after treatment in the resistant group (all  $P < 0.05$ , **Fig. 2D, 2E**). Thus, the *PPP1R14A* gene may be a key gene contributing to resistance to nivolumab in HNSCC patients, which deserves further investigation.

### *PPP1R14A* gene expression is related to low immune response

The patients were categorized into high and low expression groups according to the median of *PPP1R14A* gene expression. The ESTIAMTE algorithm analysis re-

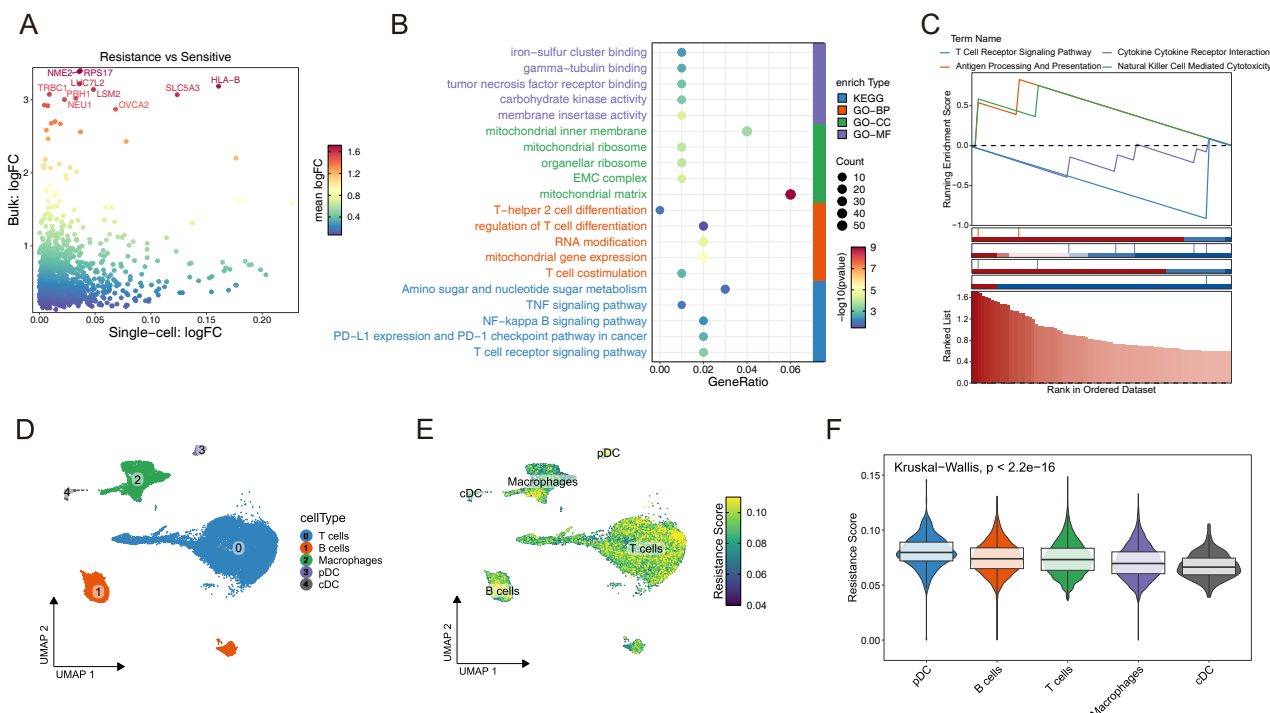


**Figure 1. Identification of nivolumab resistance-associated differentially expressed genes (DEGs) between nivolumab resistant and sensitive patients in the Gene Expression Omnibus (GEO) database.** (A) Volcano plot of DEGs between nivolumab resistant and sensitive patients in single-cell and bulk RNA-seq data. (B) Gene Ontology (GO) and Kyoto Encyclopedia of Genes and Genomes (KEGG) enrichment analyses of function annotation of DEGs. (C) Gene set enrichment analysis (GSEA) of biological function of DEGs. (D) The Uniform Manifold Approximation and Projection (UMAP) method shows the distribution of five immune-infiltrating cells in tumor tissues. (E, F) Scatter plot (E) and violin plot (F) of resistance-related scores for five immune-infiltrating cells in tumor tissues ( $n = 26,324$ ).

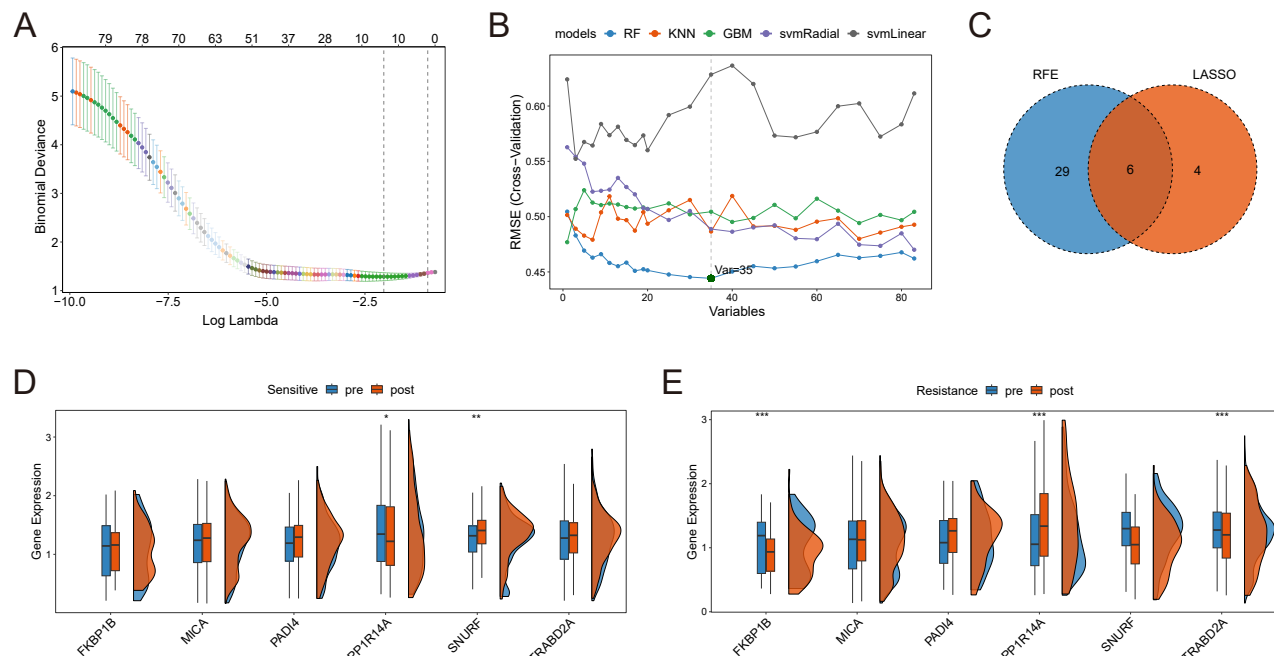


**Figure 2. Identification of key genes for drug resistance.** (A, B) Screening of key genes for drug resistance using the Least Absolute Shrinkage and Selection Operator (LASSO) regression analysis (A) and Recursive Feature Elimination (RFE) algorithm analysis (B). (C) Venn diagram shows overlapping DEGs identified by RFE and LASSO. (D, E) Comparisons of expression of each key gene in the sensitive patients (D,  $n = 42$ ) and the resistant patients (E,  $n = 54$ ) before and after nivolumab immunotherapy. \*\*\* $P < 0.001$ , \*\* $P < 0.01$ , \* $P < 0.05$ .

vealed that tumor purity was significantly higher in the *PPP1R14A* high expression group, and immune score was significantly lower ( $P < 0.05$ , **Fig. 3A**). And the expression of *PPP1R14A* gene was positively correlated with the infiltration level of memory B cells ( $r > 0$ ,  $P < 0.001$ ) and M2 macrophages ( $r > 0$ ,  $P < 0.001$ ), while negatively correlated with the infiltration of naive B cells ( $r < 0$ ,  $P < 0.001$ ) and resting CD4 memory T cells ( $r < 0$ ,  $P < 0.001$ ) (**Fig. 3B**). Besides, the *PPP1R14A* gene expression was positively correlated with the expression of immunosuppressive factors such as *PDCD1*, *CTLA4*, and *PDCD1LG2* ( $r > 0$ ,  $\log FC > 0$ ,  $OR > 1$ ,  $P < 0.05$ ; **Fig. 3C**).

These results suggested that *PPP1R14A* gene may promote drug resistance by suppressing the body's immune response to the tumor. Therefore, we further explored the relationship between *PPP1R14A*

expression and immune infiltration microenvironment of HNSCC tissues using single-cell data. As shown in **Fig. 3D**, the *PPP1R14A* gene was predominantly expressed in T cells, followed by B cells, with the lowest expression in cDC ( $P < 0.001$ ). Further analysis showed that *PPP1R14A* expression in the T cells from nivolumab resistant patients was significantly higher than that from nivolumab sensitive patients, which indicated that *PPP1R14A* gene induced immunotherapy resistance is mainly regulated by activating its expression in T cells (**Fig. 3E**). Furthermore, *PPP1R14A* gene expression in T cell subtypes was explored, and Uniform Manifold Approximation and Projection (UMAP) clustering indentified three T cell subtypes, including CD8+ T cells, CD4+ T cells, and regulatory T cells (Tregs) (**Fig. 3F**). The ratio of Tregs was lower in the nivolumab resistance group compared with the niv-

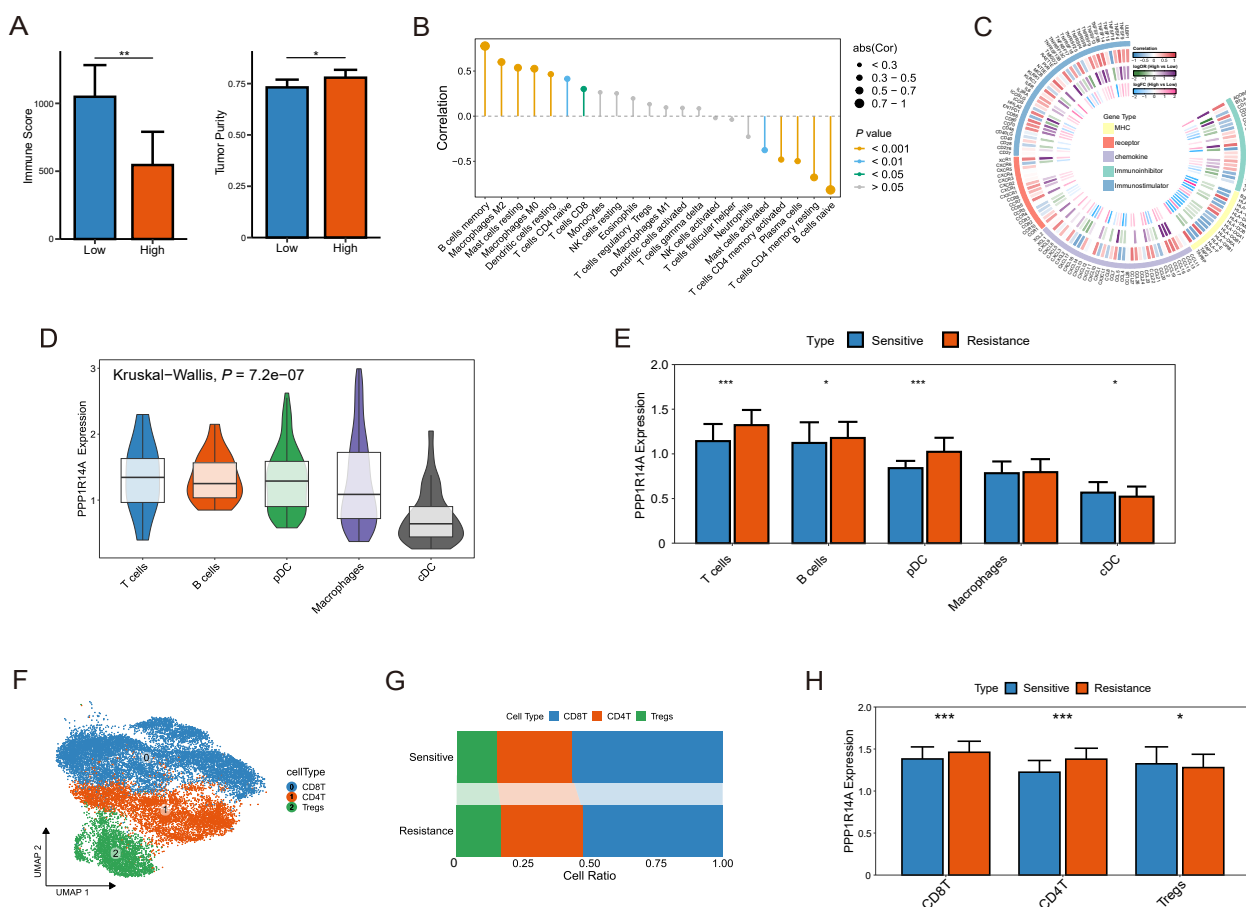


**Figure 3. Correlation of *PPP1R14A* gene expression and immune response.** (A) Differences in tumor purity and immune score between the high and low *PPP1R14A* gene expression groups ( $n = 96$ ,  $*P < 0.05$ ,  $**P < 0.01$ ). (B) Correlation between *PPP1R14A* expression and immune cell infiltration. (C) Heatmap of the correlation between *PPP1R14A* gene and immunoregulatory genes. (D) Expression of *PPP1R14A* gene in five types of immune cells ( $n = 9,347$ ). (E) Comparisons of *PPP1R14A* gene expression in five immune cell subtypes between the nivolumab resistant group and the nivolumab sensitive group ( $n = 9,347$ ,  $*P < 0.05$ ,  $***P < 0.001$ ). (F) Scatter plot of UMAP distribution of T cell subtypes. (G) Proportion of T cells in different immunotherapy response groups ( $\chi^2 = 33.56$ ,  $P < 0.001$ ). (H) Differential *PPP1R14A* expression in CD8+ cells, CD4+ cells, and regulatory T cells (Tregs) in the immunotherapy sensitive and resistant groups. ( $*P < 0.05$ ,  $**P < 0.001$ ).

olumab sensitive group, while the ratios of CD4+ T cells and CD8+ T cells were higher ( $P < 0.001$ , **Fig. 3G**). Further, compared with the nivolumab-sensitive group, *PPP1R14A* expression level was higher in the anti-tumor immune cells such as CD8+ T cells and CD4+ T cells of the nivolumab-resistant group, while the expression level was lower in the pro-tumor im-

mune cells like Tregs cells ( $P < 0.05$ , **Fig. 3H**).

### Functional enrichment of *PPP1R14A*

GSVA showed that signaling pathways such as amino acid metabolism, glucose metabolism, biosynthesis and metabolism of glycan, and lipid metabolism had significant difference between the high and low *PPP1R14A* expression groups (**Fig. 4A**). More-

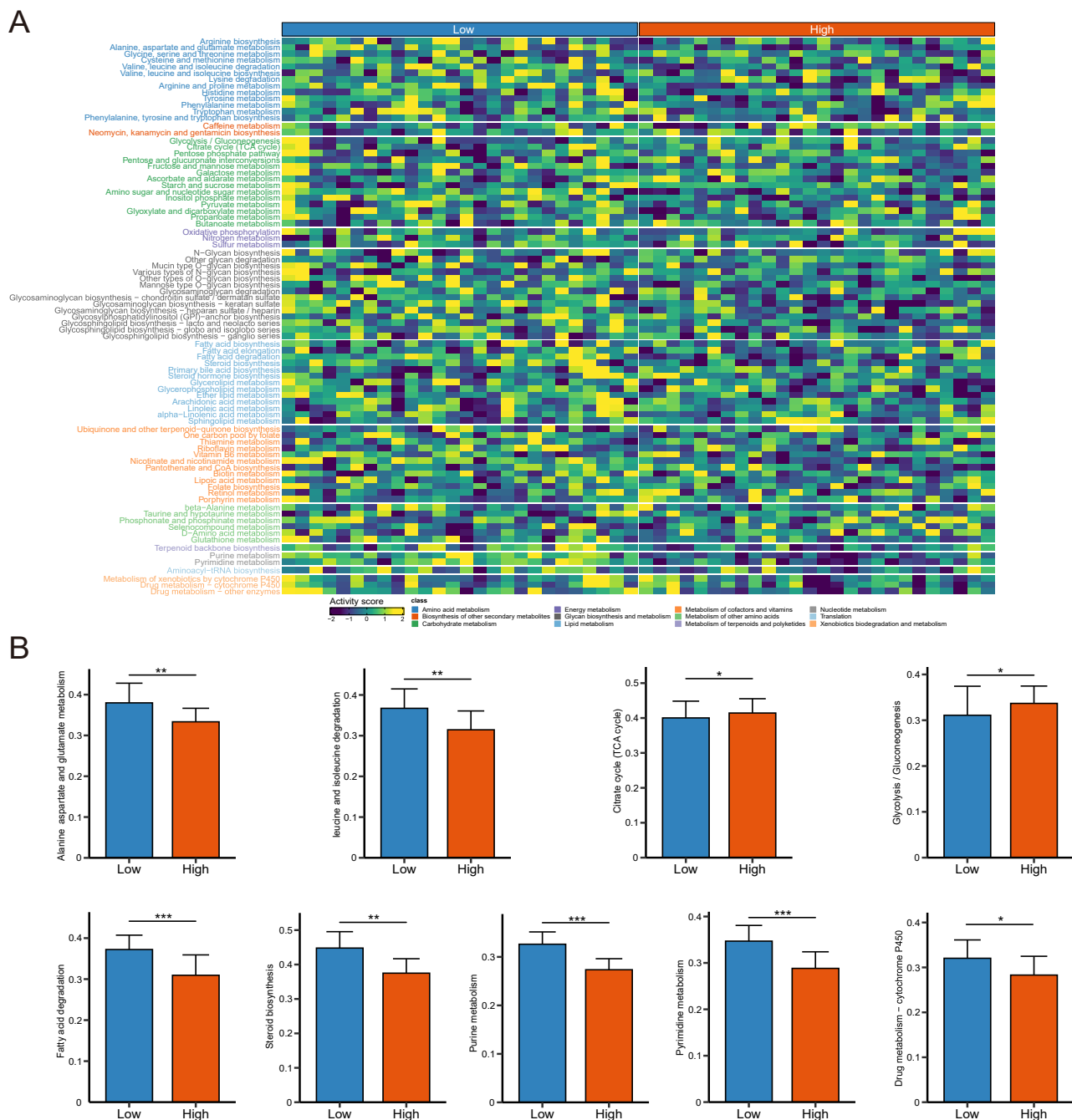


**Figure 4. The function enrichment of *PPP1R14A*.** (A) Heatmap of gene set variation analysis (GSVA) scores for 84 metabolism pathways in the high and low *PPP1R14A* expression groups. (B) Distribution of GSVA scores of different metabolism pathways in the high and low *PPP1R14A* expression groups ( $n = 53$ , \* $P < 0.05$ , \*\* $P < 0.01$ , \*\*\* $P < 0.001$ ).

over, quantitative analysis showed that the highly expressed *PPP1R14A* was mainly enriched in tricarboxylic acid cycle and glycolytic pathway. While, the lowerly expressed *PPP1R14A* was mainly enriched in pathways of alanine, aspartate and glutamate metabolism, leucine and isoleucine degradation, fatty acid degradation, steroid biosynthesis, purine and pyrimidine metabolism, and drug metabolism (**Fig. 4B**).

### Pseudotime and cellular communication of immune cells

CytoTRACE and Monocle3 identified pseudotime scores for four cell clusters, including dendritic cells, macrophages, T cells, and B cells, infiltrated in the tumor tissues. Dendritic cells and macrophages were identified as a low differentiated state (**Fig. 5A, 5B**). Immune cells in the high *PPP1R14A* gene expression group had lower differentiation (**Fig. 5C, 5D**).

CellChat analysis showed that the intensity of ligand-receptor interaction between the HLA family and CD4 in the high *PPP1R14A* group was higher than

that of other ligand-receptor pairs in the low *PPP1R14A* expression groups (**Fig. 5E**). Furthermore, the signaling pathways regulating HLA-CD4 interactions, MHC-I, and MHC-II were activated in the high *PPP1R14A* expression group (**Fig. 5F**).

### Potentially sensitive drug

As shown in **Fig. 6**, among 565 drugs screened in the bulk sequencing data, the IC<sub>50</sub> value of AXITINIB showed the greatest negative correlation with the expression of *PPP1R14A* (**Fig. 6A**). Screening of the single-cell sequencing data also confirmed that the IC<sub>50</sub> value of AXITINIB in the *PPP1R14A* high-expression group was smaller than that in the low-expression group (**Fig. 6B, 6C**). Furthermore, at the cellular level, T cells had the lowest sensitivity to AXITINIB, but pDC had the highest sensitivity (**Fig. 6D**).

### Validation of *PPP1R14A* expression in TCGA data-set cohorts

Patients in the TCGA cohort were divided into nivolumab sensitive ( $n = 209$ ) and resistant groups ( $n =$

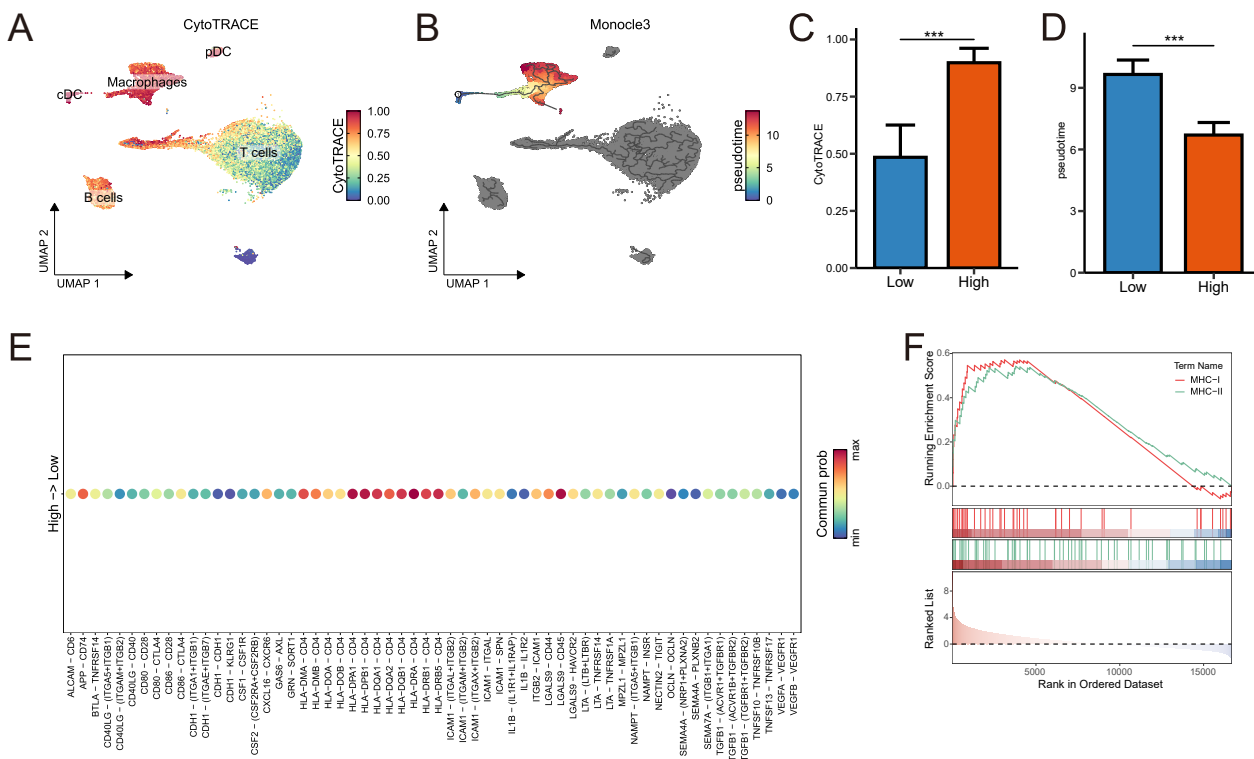


**Figure 5. Identification of pseudotime and cellular communication of immune cells infiltrated in tumor tissues on single cell dataset.** (A) Cellular heterogeneity identification with CytoTRACE method. (B) Cellular heterogeneity identification with Monocle3. (C, D) Comparisons of CytoTRACE score (C) and pseudotime score (D) between the high and low *PPP1R14A* gene expression groups ( $^{***}P < 0.001$ ). (E) Potential ligand-receptor communication associated with *PPP1R14A*. (F) GSEA analysis of the MHC-I and MHC-II pathways associated with *PPP1R14A* expression.

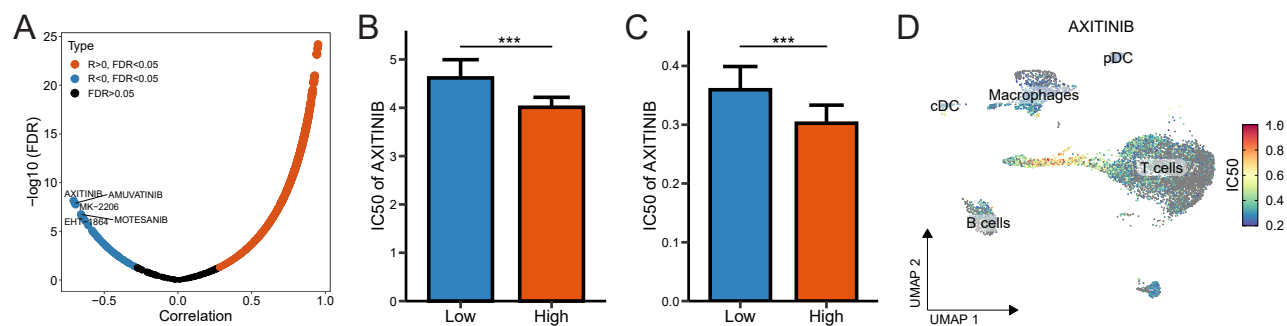


**Figure 6. Screening potentially sensitive drug for nivolumab resistant HNSCC patients.** (A) The correlation between *PPP1R14A* gene expression and the half maximal inhibitory concentration (IC50) of 565 FDA approved immunotherapeutics. (B, C) Comparisons of IC50 of AXITINIB in bulk (B) and single-cell (C) sequencing data between the high and low *PPP1R14A* expression groups (\*\*P < 0.001). (D) Scatter plots of IC50 of AXITINIB for immune cells.

313) (**Fig. 7A**). *PPP1R14A* gene expression was positively correlated with tumor immune dysfunction and exclusion (TIDE) scores ( $r > 0$ ,  $P < 0.05$ , **Fig. 7B**), and *PPP1R14A* gene was significantly highly expressed in the nivolumab resistant group compared with the sensitive group ( $P < 0.05$ , **Fig. 7C**). Similarly, there was a significant difference in HNSCC patients' immunotherapy response between the two *PPP1R14A* gene expression groups, with lower benefit in the high expression group ( $P < 0.05$ , **Fig. 7D**). This further demonstrates that *PPP1R14A* gene is expected to be a target for predicting immunotherapy resistance in HNSCC patients. Moreover, we validated this findings in the GSE212551 and GSE226134 cohorts of HNSCC patients, and the results supported our findings as well (**Fig. 7C, 7D**).

## DISCUSSION

The rich blood supply and dense lymphatic tissues in the head and neck lead to HNSCC susceptible to invasion and metastasis, and the therapeutic effect is unsatisfactory<sup>[25]</sup>. Currently, cisplatin is the adjuvant therapeutic choice for patients with advanced localized HNSCC. However, due to the prolonged platinum exposure, patients are prone to drug resistance<sup>[26]</sup>. Immunotherapy, an emerging oncology therapy with unprecedented efficacy against a wide range of tumors, has been approved for the treatment of HNSCC recurrence or metastasis during or after platinum-based therapy<sup>[27-29]</sup>. Although immunotherapy has dramatically improved the prognosis of patients with advanced HNSCC, only 20%–30% of treated patients benefit in the long term, which may be attributed to drug resistance due to dysfunction or down-regulation of

antigen presentation, depletion of expressed tumor neoantigens, and tumor-mediated immune rejection<sup>[30,31]</sup>. Hence, exploring how resistance to immunotherapy in HNSCC arises and develops and what its molecular targets are is necessary to improve prognosis of HNSCC patients. In this study, we revealed a significant relationship between *PPP1R14A* gene and resistance to nivolumab in HNSCC patients through analyzing bulk and single-cell sequencing data.

We identified that after nivolumab treatment the expression of *PPP1R14A* gene was increased in the immunotherapy-resistant patients and decreased in the sensitive patients. This suggests that *PPP1R14A* may associated with drug resistance in HNSCC patients. *PPP1R14A* may be a promoter of the infiltration of pro-tumor immune microenvironment cells, such as M2 macrophages, resting mast cells, and memory B cells. The infiltration of these immune cells has been shown to be involved in the progression of HNSCC<sup>[32-34]</sup>. Moreover, *PPP1R14A* gene may also be activated by immunosuppressive factors such as *PDCD1*, *CTLA4* and *PDCD1LG2*, which are participated in HNSCC progression.

The human *PPP1R14A* gene is localized at 19q13.1 and encodes a protein containing 147 amino acids<sup>[35]</sup>. The Human Protein Atlas (HPA) database shows that *PPP1R14A* protein is mainly localized in the nucleoplasm and to a less extent in nucleosomes<sup>[36]</sup>. It belongs to the protein phosphatase 1 inhibitor family and acts as an important regulator of protein phosphorylation. It regulates a variety of cellular processes, such as actin contraction, glycogen metabolism, cell cycle, protein synthesis, and neuronal signal transduction<sup>[37]</sup>. Previous studies have found that *PPP1R14A* is associated with the development of various diseases,

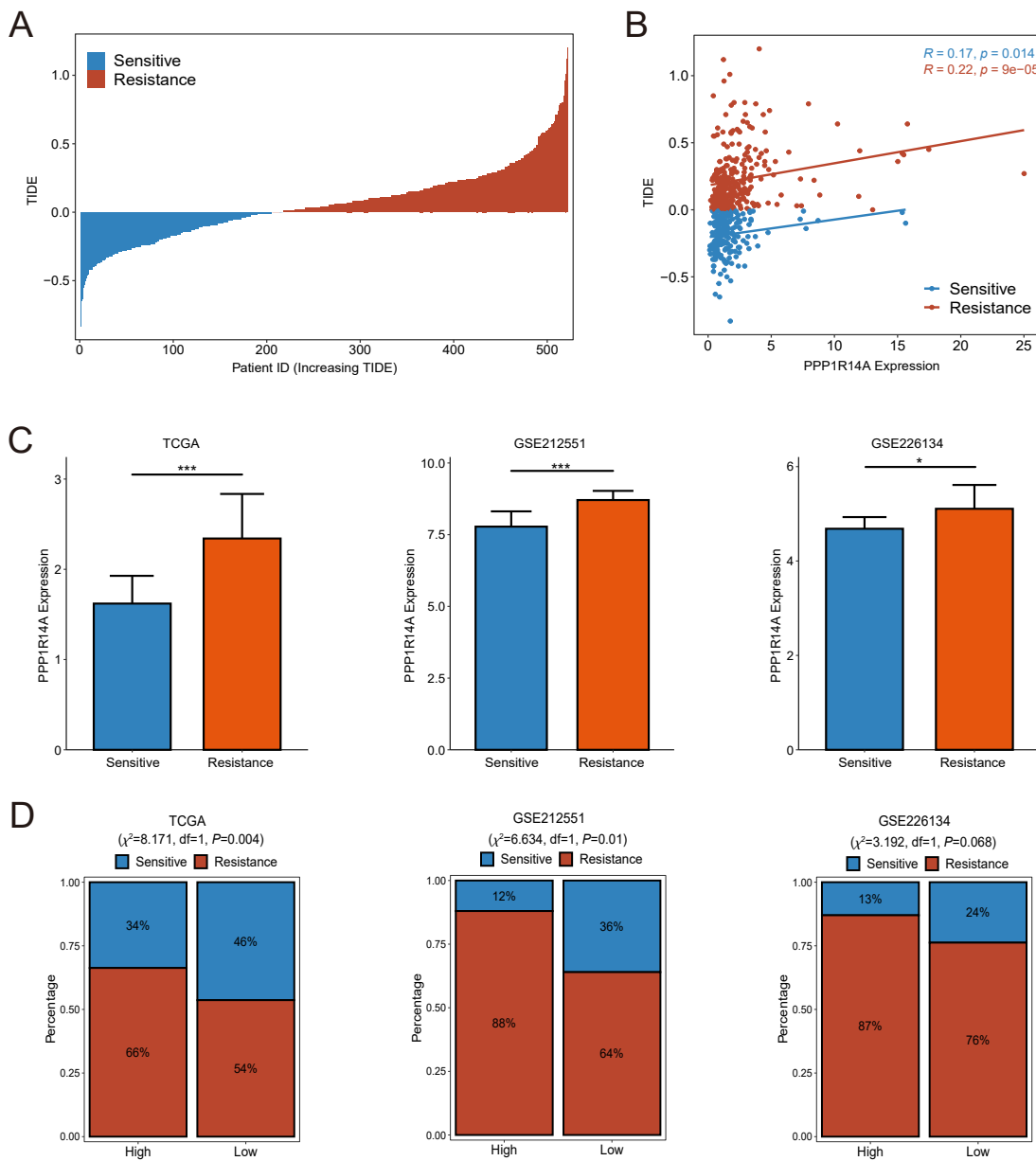


**Figure 7. Validation of PPP1R14A expression in external cohorts.** (A) The tumor immune dysfunction and exclusion (TIDE) score distribution of the TCGA cohort samples. (B) Correlation between the PPP1R14A expression and TIDE scores in the nivolumab-sensitive and -resistant groups. (C) Differential PPP1R14A expression in nivolumab-sensitive and -resistant groups in the TCGA ( $n = 552$ ), GSE212551 ( $n = 100$ ), and GSE226134 ( $n = 49$ ) cohorts. (\* $P < 0.05$ , \*\*\* $P < 0.001$ ). (D) Relationship between PPP1R14A expression and immunotherapy response in the TCGA, GSE212551, and GSE226134 cohorts.

including prostate cancer, cervical cancer, and Alzheimer's disease<sup>[38-40]</sup>.

It has been proved that cellular metabolic processes are involved in tumor immunotherapy resistance<sup>[41]</sup>. To clarify whether metabolism-related pathways participated in immunotherapeutic resistance in HNSCC patients, we analyzed single-cell and bulk RNA-sequencing data using bioinformatic analysis,

and verified that a significant relationship between high PPP1R14A expression and activation of tricarboxylic acid cycle and glycolysis. The study by Liu *et al.*<sup>[42]</sup> also confirmed that inhibiting tricarboxylic acid cycle can enhance the efficacy of anti-PD1 therapy in melanoma patients. Furthermore, we found higher PPP1R14A expression mediated immunotherapy resistance in HNSCC patients by inhibiting amino acid me-

tabolism. In tumor immune microenvironment, amino acid metabolism has been proved to regulate the proliferation and anti-tumor activity of T cells, NK cells, and B cells<sup>[43]</sup>. Therefore, *PPP1R14A* may promote nivolumab resistance by regulating metabolism pathways in tumor tissues, such as the tricarboxylic acid cycle, glycolysis, and amino acid metabolism.

In addition, high *PPP1R14A* gene expression was closely associated with cell stemness and increased with the progression of cell differentiation. The role of high cell stemness in HNSCC heterogeneity, metastasis, and cisplatin resistance has been demonstrated and may have a potential impact on immunotherapy resistance<sup>[44]</sup>. Our research identified AXITINIB as one of the potential therapeutic agents for patients resistant to nivolumab. AXITINIB is a multi-tyrosine kinase inhibitor whose targets include VEGFR-1, -2, and -3. In addition, it has inhibitory activity against the downstream effectors of PDGFR and EGFR, both of which usually contribute to head and neck tumorigenesis<sup>[45]</sup>. In cisplatin-resistant patients with advanced recurrent or metastatic HNSCC, the 6-month overall survival rate was found to be 70% in patients treated with AXITINIB, which was higher than that of the control group (50%), and the combination of AXITINIB with an anti-PD-1 drug further improved the overall survival rate of HNSCC patients<sup>[46]</sup>.

In conclusion, we screened out the genes associated with resistance to nivolumab in HNSCC patients by single-cell and bulk RNA-sequencing data and explored how these genes contribute to immunotherapeutic resistance. However, our study had limitations. First, although we performed bioinformatic analysis of two types of sequencing data, a much larger sample is still needed to confirm this findings. Second, the single-cell dataset we analyzed only contained immune cells but did not contain tumor cells. Finally, the study lacked experimental validation of the bioinformatic results.

## ARTICLE INFORMATION

### Conflict of interests

The authors declare no conflict of interests.

### Authors' contributions

All authors contributed to the conceptualization and design of the study. Data collection and analysis were performed by Ma

JJ and Zhang L. The manuscript was drafted by Ma JJ and revised by Lu J and Zhang HX. All authors read and approved the final manuscript.

### Funding

This study was supported by the National Innovation and Entrepreneurship Training Program for College Students (202210367002) and the Key Laboratory Open Project of Anhui Province (AHCM2022Z004).

### Data availability

The data used in the manuscript can be found in the GEO and TCGA databases. Data analysis codes are available by contacting the corresponding author.

## REFERENCES

- Zhao X, Mai Z, Liu L, et al. Hypoxia-driven TNS4 fosters HNSCC tumorigenesis by stabilizing integrin α5β1 complex and triggering FAK-mediated Akt and TGFβ signaling pathways. *Int J Biol Sci* 2024; 20(1): 231-48. doi: 10.7150/ijbs.86317.
- Guo X, Xu L, Nie L, et al. B cells in head and neck squamous cell carcinoma: current opinion and novel therapy. *Cancer Cell Int* 2024; 24(1): 41. doi: 10.1186/s12935-024-03218-3.
- Mathan SV, Singh R, Kim SH, et al. Diallyl trisulfide induces ROS-mediated mitotic arrest and apoptosis and inhibits HNSCC tumor growth and cancer stemness. *Cancers (Basel)* 2024; 16(2): 378. doi: 10.3390/cancers16020378.
- Liu S, Wang R, Fang J. Exploring the frontiers: tumor immune microenvironment and immunotherapy in head and neck squamous cell carcinoma. *Discov Oncol* 2024; 15(1):22. doi: 10.1007/s12672-024-00870-z.
- Gong X, Xiong J, Gong Y, et al. Deciphering the role of HPV-mediated metabolic regulation in shaping the tumor microenvironment and its implications for immunotherapy in HNSCC. *Front Immunol* 2023; 14: 1275270. doi: 10.3389/fimmu.2023.1275270.
- Li C, Guo H, Zhai P, et al. Spatial and single-cell transcriptomics reveal a cancer-associated fibroblast subset in HNSCC that restricts infiltration and antitumor activity of CD8+ T cells. *Cancer Res* 2024; 84(2): 258-75. doi: 10.1158/0008-5472.CAN-23-1448.
- Han X, Zhang H, Sun K, et al. Durvalumab with or without tremelimumab for patients with recurrent or metastatic squamous cell carcinoma of the head and neck: a systematic review and meta-analysis. *Front Immunol* 2023; 14:1302840. doi: 10.3389/fimmu.2023.1302840.
- Ritchie ME, Phipson B, Wu D, et al. limma powers differential expression analyses for RNA-sequencing and microarray studies. *Nucleic Acids Res* 2015; 43(7):e47. doi: 10.1093/nar/gkv007.
- Stuart T, Butler A, Hoffman P, et al. Comprehensive integration of single-cell data. *Cell* 2019; 177(7):1888-902.e21. doi: 10.1016/j.cell.2019.05.031.
- Andreatta M, Carmona SJ. UCell: robust and scalable single-cell gene signature scoring. *Comput Struct Biotechnol J* 2021; 19: 3796-8. doi: 10.1016/j.csbj.2021.06.043.
- Wu T, Hu E, Xu S, et al. clusterProfiler 4.0: a universal enrichment tool for interpreting omics data. *Innovation (Camb)* 2021; 2(3): 100141. doi: 10.1016/j.xinn.2021.100141.
- Subramanian A, Tamayo P, Mootha VK, et al. Gene set enrichment analysis: a knowledge-based approach for interpreting genome-wide expression profiles. *Proc Natl Acad Sci USA* 2005; 102(43): 15545-50. doi: 10.1073/pnas.0506580102.
- Hänzelmann S, Castelo R, Guinney J. GSVA: gene set variation analysis for microarray and RNA-seq data. *BMC Bioinformatics* 2013; 14: 7. doi: 10.1186/1471-2105-14-7.

- 10.1186/1471-2105-14-7.
14. Tibshirani R. Regression shrinkage and selection via the Lasso. *J Royal Statistical Society: Series B (Methodological)* 1996; 58(1):267-88.
  15. Han Y, Huang L, Zhou F. A dynamic recursive feature elimination framework (dRFE) to further refine a set of OMIC biomarkers. *Bioinformatics* 2021; 37(15):2183-9. doi: 10.1093/bioinformatics/btab055.
  16. Newman AM, Liu CL, Green MR, et al. Robust enumeration of cell subsets from tissue expression profiles. *Nat Methods* 2015; 12(5):453-7. doi: 10.1038/nmeth.3337.
  17. Yoshihara K, Shahmoradgoli M, Martínez E, et al. Inferring tumour purity and stromal and immune cell admixture from expression data. *Nat Commun* 2013; 4:2612. doi: 10.1038/ncomms3612.
  18. Gulati GS, Sikandar SS, Wescche DJ, et al. Single-cell transcriptional diversity is a hallmark of developmental potential. *Science* 2020; 367(6476):405-11. doi: 10.1126/science.aax0249.
  19. Cao J, Spielmann M, Qiu X, et al. The single-cell transcriptional landscape of mammalian organogenesis. *Nature* 2019; 566(7745):496-502. doi: 10.1038/s41586-019-0969-x.
  20. Lai Y, Lu X, Liao Y, et al. Crosstalk between glioblastoma and tumor microenvironment drives proneural-mesenchymal transition through ligand-receptor interactions. *Genes Dis* 2024; 11(2):874-89. doi: 10.1016/j.gendis.2023.05.025.
  21. Jin S, Guerrero-Juarez CF, Zhang L, et al. Inference and analysis of cell-cell communication using CellChat. *Nat Commun* 2021; 12(1): 1088. doi: 10.1038/s41467-021-21246-9.
  22. Maeser D, Gruener RF, Huang RS. oncoPredict: an R package for predicting *in vivo* or cancer patient drug response and biomarkers from cell line screening data. *Brief Bioinform* 2021; 22(6): bbab260. doi: 10.1093/bib/bbab260.
  23. Fustero-Torre C, Jiménez-Santos MJ, García-Martín S, et al. Beyondcell: targeting cancer therapeutic heterogeneity in single-cell RNA-seq data. *Genome Med* 2021; 13(1):187. doi: 10.1186/s13073-021-01001-x.
  24. Fu J, Li K, Zhang W, et al. Large-scale public data reuse to model immunotherapy response and resistance. *Genome Med* 2020; 12(1):21. doi: 10.1186/s13073-020-0721-z.
  25. Zhao X, Guo B, Sun W, et al. Targeting squalene epoxidase confers metabolic vulnerability and overcomes chemoresistance in HNSCC. *Adv Sci (Weinh)* 2023; 10(27):e2206878. doi: 10.1002/advs.202206878.
  26. Guo Y, Nakashima T, Cho BC, et al. Clinical decision pathway and management of locally advanced head and neck squamous cell carcinoma: a multidisciplinary consensus in Asia-Pacific. *Oral Oncol* 2024; 148: 106657. doi: 10.1016/j.oraloncology.2023.106657.
  27. Runnels J, Bloom JR, Hsieh K, et al. Combining radiotherapy and immunotherapy in head and neck cancer. *Biomedicines* 2023; 11(8): 2097. doi: 10.3390/biomedicines11082097.
  28. Zhang J, Joshua AM, Li Y, et al. Targeted therapy, immunotherapy, and small molecules and peptidomimetics as emerging immunoregulatory agents for melanoma. *Cancer Lett* 2024; 586:216633. doi: 10.1016/j.canlet.2024.216633.
  29. Yin J, Gu T, Chaudhry N, et al. Epigenetic modulation of antitumor immunity and immunotherapy response in breast cancer: biological mechanisms and clinical implications. *Front Immunol* 2023; 14: 1325615. doi: 10.3389/fimmu.2023.1325615.
  30. Iwasa YI, Nakajima T, Hori K, et al. A spatial transcriptome reveals changes in tumor and tumor microenvironment in oral cancer with acquired resistance to immunotherapy. *Biomolecules* 2023; 13(12):1685. doi: 10.3390/biom13121685.
  31. Meliante PG, Zoccali F, de Vincentiis M, et al. Diagnostic predictors of immunotherapy response in head and neck squamous cell carcinoma. *Diagnostics (Basel)* 2023; 13(5):862. doi: 10.3390/diagnostics13050862.
  32. Wei F, Fang R, Lyu K, et al. Exosomal PD-L1 derived from head and neck squamous cell carcinoma promotes immune evasion by activating the positive feedback loop of activated regulatory T cell-M2 macrophage. *Oral Oncol* 2023; 145:106532. doi: 10.1016/j.oraloncology.2023.106532.
  33. Jin Y, Qin X. Profiles of immune cell infiltration and their clinical significance in head and neck squamous cell carcinoma. *Int Immunopharmacol* 2020; 82:106364. doi: 10.1016/j.intimp.2020.106364.
  34. Bao J, Betzler AC, Hess J, et al. Exploring the dual role of B cells in solid tumors: implications for head and neck squamous cell carcinoma. *Front Immunol* 2023; 14:1233085. doi: 10.3389/fimmu.2023.1233085.
  35. Stelzer G, Rosen N, Plaschkes I, et al. The GeneCards suite: from gene data mining to disease genome sequence analyses. *Curr Protoc Bioinformatics* 2016; 54:1.30.1-1.30.33. doi: 10.1002/cpb1.5.
  36. Thul PJ, Akesson L, Wiklund M, et al. A subcellular map of the human proteome. *Science* 2017; 356(6340):eaal3321. doi: 10.1126/science.aal3321.
  37. Wang Z, Huang R, Wang H, et al. Prognostic and immunological role of PPP1R14A as a Pan-cancer analysis candidate. *Front Genet* 2022; 13: 842975. doi: 10.3389/fgene.2022.842975.
  38. Tian Y, Soupir A, Liu Q, et al. Novel role of prostate cancer risk variant rs7247241 on PPP1R14A isoform transition through allelic TF binding and CpG methylation. *Hum Mol Genet* 2022; 31(10):1610-21. doi: 10.1093/hmg/ddab347.
  39. Liu L, Zhu H, Wang P, et al. Construction of a six-gene prognostic risk model related to hypoxia and angiogenesis for cervical cancer. *Front Genet* 2022; 13:923263. doi: 10.3389/fgene.2022.923263.
  40. Yu QS, Feng WQ, Shi LL, et al. Integrated analysis of cortex single-cell transcriptome and serum proteome reveals the novel biomarkers in Alzheimer's disease. *Brain Sci* 2022; 12(8):1022. doi: 10.3390/brainsci12081022.
  41. Zou W, Green DR. Beggars banquet: Metabolism in the tumor immune microenvironment and cancer therapy. *Cell Metab* 2023; 35(7):1101-13. doi: 10.1016/j.cmet.2023.06.003.
  42. Liu N, Yan M, Tao Q, et al. Inhibition of TCA cycle improves the anti-PD-1 immunotherapy efficacy in melanoma cells via ATF3-mediated PD-L1 expression and glycolysis. *J Immunother Cancer* 2023; 11(9):e007146. doi: 10.1136/jitc-2023-007146.
  43. Yang L, Chu Z, Liu M, et al. Amino acid metabolism in immune cells: essential regulators of the effector functions, and promising opportunities to enhance cancer immunotherapy. *J Hematol Oncol* 2023; 16(1):59. doi: 10.1186/s13045-023-01453-1.
  44. Liu Y, Li S, Wang S, et al. LIMP-2 enhances cancer stem-like cell properties by promoting autophagy-induced GSK3 $\beta$  degradation in head and neck squamous cell carcinoma. *Int J Oral Sci* 2023; 15(1):24. doi: 10.1038/s41368-023-00229-0.
  45. Swiecicki PL, Spector M, Worden FP. Axitinib in the treatment of head and neck malignancies. *Curr Clin Pharmacol* 2016; 11(2):72-6. doi: 10.2174/1574884711666160518120622.
  46. Swiecicki PL, Bellile EL, Brummel CV, et al. Efficacy of axitinib in metastatic head and neck cancer with novel radiographic response criteria. *Cancer* 2021; 127(2):219-28. doi: 10.1002/cncr.33226.

(Edited by Jun-Ying Yao)